Titu Maiorescu University

DOCTORAL SCHOOL

FIELD OF MEDICINE

DOCTORAL THESIS (SUMMARY)

INNOVATIVE ASPECTS REGARDING IMPLANTS USED IN ORTHOPEDIC CONDITIONS FROM THE PERSPECTIVE OF BIOMATERIALS

PhD Coordinator: Prof. Univ. Dr. MARIUS NICULESCU

PhD Candidate: CORDUNIANU MIHAI ALEXANDRU

Bucharest 2024

TABLE OF CONTENTS

INTRODUCTION

Medical devices, including orthopedic implants, are essential for improving patients' quality of life, especially for those suffering from bone fractures caused by sports activities or road accidents—an increasingly common issue among the young and adult population. Among the methods used to stabilize bone fractures, osteosynthesis materials such as fixation plates, screws, and rods represent a standard therapeutic approach in orthopedic surgery. These implants must meet fundamental criteria, such as promoting bone healing and minimizing the risk of local or systemic adverse reactions.

The materials used to manufacture osteosynthesis devices are typically biocompatible metal alloys. However, significant differences between their elasticity modulus and that of the bone can lead to complications. This stiffness mismatch may result in stress shielding, a phenomenon where improper mechanical load distribution on the bone decreases local bone stimulation, potentially causing bone resorption near the implant and loss of stability. Therefore, selecting materials with an elasticity modulus closer to that of native bone is crucial for promoting bone healing and maintaining long-term implant stability. Additionally, other important aspects include the biocompatibility of the alloys with human tissues, resistance to corrosion, and the ability to stimulate osseointegration and bone proliferation. The development of biocompatible materials for osteosynthesis has been a key factor in advancing orthopedic treatments, making these materials a central component of modern surgical interventions. Orthopedic implants are continually evolving, aiming to offer improved clinical outcomes while reducing associated risks and costs. A significant innovation in this field is the emergence of biodegradable implants. Although the use of these implants is still in its early stages, they have the potential to fundamentally transform the management of orthopedic conditions by eliminating the need for surgical procedures to remove osteosynthesis materials.

This study provides a detailed and objective analysis of implants used in treating traumatic and chronic pathologies of the upper and lower limbs. The present research aims to evaluate the behavior of orthopedic implants under specific conditions and identify the causes leading to their failure, with the primary objective of improving the osseointegration process and reducing associated mechanical and biological complications. The studied implants include rods, plates, and screws of various shapes, sizes, and functionalities.

Microstructural characterization will be performed using a scanning electron microscope (SEM) equipped with an energy-dispersive X-ray spectrometer (EDS), Phenom ProX model (PhenomWorld, Eindhoven, Netherlands). Surface roughness analysis will be conducted using profilometry with the Form Talysurf® i-Series PRO Range device (Taylor Hobson, Leicester, UK), and the contact angle will be determined using a KRUSS DSA 30 optical tensiometer (Hamburg, Germany). Medical imaging plays a crucial role in evaluating fractures and monitoring the stability of implants in the human body. In this study, radiography and computed tomography (CT) are used as the main investigation methods.

To assess the functional efficacy of these implants, multiple clinical and preclinical studies have been conducted, demonstrating that these implants can be used in routine medical practice. The results of these investigations have highlighted the importance of proper design and surface adaptation of implants to achieve superior clinical performance, thereby contributing to the development of advanced therapeutic solutions in orthopedic surgery.

The structure of this doctoral thesis is as follows:

THEORETICAL PART

Chapter 1 – "General Considerations Regarding the Anatomy and Biomechanics of the Bone System" addresses general aspects of human hard tissues, focusing on the structure and functions of bone.

Chapter 2 – "The Use of Metal Implants in Traumatology" is divided into four subsections and provides an in-depth presentation of essential aspects related to implants and their use in treating orthopedic injuries. It comprehensively discusses the various types of orthopedic conditions that may arise from different causes and the associated therapeutic strategies. Additionally, the main categories of metal implants are described, highlighting their properties and role in stabilizing and restoring bone fractures. Finally, the biological mechanisms by which implants interact with bone tissue are detailed, with a particular focus on the processes of osseointegration and bone healing in the presence of an implant.

SPECIAL PART

Chapter 3 – "Innovative Elements Regarding Metallic Biomaterials Used in the Manufacturing of Metallic Implants for Traumatology" discusses recent advances in modifying the surfaces of titanium metal implants to improve biocompatibility and osseointegration, as well as the use

of biodegradable magnesium alloys as a promising alternative due to their ability to degrade in a controlled manner in the body, eliminating the need for surgical implant removal.

Chapter 4 – “Experimental Evaluation of the Surface Properties of Metallic Implants Used in Traumatology” presents experimental determinations regarding the surface properties that influence fracture stabilization.

Chapter 5 – “Development of an Experimental Analysis Protocol for Metallic Implants Used in Traumatology After Their Failure” details the steps to determine the causes of implant failures.

Chapter 6 – “Conclusions and Personal Contributions” offers both a general summary and a presentation of the original contributions and dissemination of the obtained results. Finally, the bibliography, a table index, and a figure index are included.

CHAPTER 4: EXPERIMENTAL EVALUATION OF THE SURFACE PROPERTIES OF METALLIC IMPLANTS USED IN TRAUMATOLOGY

4.1. PURPOSE OF THE STUDY, EXPERIMENTAL MATERIALS, AND WORK PLAN

In this subchapter of the doctoral thesis, the primary objectives were to analyze four osteosynthesis screws, both cannulated and non-cannulated, made of a titanium alloy (Ti6Al4V) and to evaluate the effects of their anodization, with each screw exhibiting a distinct color (gray, blue, violet, and green). It is important to note that the analysis was performed on commercially available screws, so the anodization parameters are not known. These screws were characterized and tested to determine whether the properties resulting from the anodization process correlated with the surface properties.

Anodization is a surface modification method used to enhance the properties of metals by creating an oxide layer on their surface. This layer provides protection against corrosion and wear. One notable aspect of anodization is its ability to impart orthopedic implants with a wide range of colors.

The colors obtained through anodization are referred to as interference colors. According to the specialized literature, the color variation observed on the surface of titanium and its alloys is due to the voltage applied to create titanium dioxide (TiO_2) films. The higher the applied voltage, the thicker the titanium dioxide layer, which results in better corrosion resistance [88]. Figure 4.1 illustrates the applied voltage, the color resulting from the voltage, and the thickness of the titanium dioxide layer.

To achieve the main objective of this study, several steps were undertaken:

- Selection of titanium alloys suitable as biomaterials for manufacturing osteosynthesis screws based on biofunctionality criteria.

Sample 1 – gray anodized screw

Sample 2 – blue anodized screw

Sample 3 – violet anodized screw

Sample 4 – green anodized screw

Sample 1 – gray anodized screw

Sample 2 – blue anodized screw

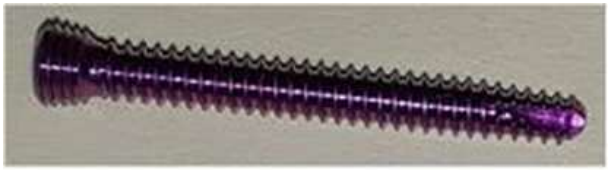

Sample 3 – violet anodized screw

Sample 4 – green anodized screw

Figure 4.2. Macro images of the anodized osteosynthesis screws

- Selection of the optimal surface modification method for the experimental titanium alloy.
- Anodization of experimental titanium alloys (Ti6Al4V).
- Determination of the surface properties of the anodized osteosynthesis screws.
- Experimental Materials Used in This Analysis: Titanium alloy, specifically anodized Ti6Al4V (Figure 4.2).

The work plan was organized into stages, based on the knowledge acquired and information obtained from the specialized literature, and is schematically presented as follows:

• Selection of titanium alloys suitable as biomaterials for the production of osteosynthesis screws based on biofunctionality criteria (a titanium alloy, specifically Ti6Al4V);

• Choosing the most suitable surface modification method for the experimental titanium alloy, specifically anodizing the experimental titanium alloy Ti6Al4V, achieved by controlled formation of an oxide layer on the metal surface (the analysis was conducted on commercial screws, so the anodizing parameters are unknown);

• Determining the surface properties of anodized osteosynthesis screws through SEM-EDS, contact angle, and roughness analysis.

4.2 METHODS OF ANALYSIS AND EQUIPMENT USED

4.2.1. SCANNING ELECTRON MICROSCOPY (SEM) AND ENERGY-DISPERSIVE X-RAY SPECTROSCOPY (EDS)

The scanning electron microscope (SEM) interacts with the sample using a focused electron beam. This produces images that reflect both the topographical structure and its relative composition. When the electron beam strikes the sample, X-rays, as well as secondary electrons, are released and backscattered. Detectors can capture these X-rays and convert them into images displayed on the monitor. A standard SEM includes an electron detector, an electron source, electromagnetic lenses, a sample chamber, and a computer display system.

To characterize the chemical composition of biomaterials, several analytical methods are employed. In this study, energy-dispersive spectroscopy (EDS) was applied to identify the chemical composition of the samples. The working principle of EDS is based on the interaction of X-rays with the sample's atoms, causing the ejection of electrons from their inner shells. The energy released during this process is specific to each chemical element, enabling their identification and quantification.One of the main advantages of SEM is its ability to provide images with extremely high resolution, allowing the analysis of microscopic details on the sample surfaces. Moreover, SEM allows depth-of-field adjustments, offering the possibility to examine surfaces at various heights.

In this study, the morphology and elemental composition of the anodized sample surfaces were examined using a scanning electron microscope equipped with an energy-dispersive X-ray spectrometer (SEM-EDS, Phenom ProX, PhenomWorld, Eindhoven, Netherlands).

4.2.2. PROFILOMETRY

A profilometer is used for the topographic analysis of solid surfaces, enabling the monitoring of microscopic surface variations of the sample. Using this technique, surface roughness can be quantified, and high-resolution images of the morphology of the studied samples can be obtained [90].

The surface roughness of anodized screws was measured using a Form Talysurf® i-Series PRO Range surface profilometer from Taylor Hobson (Leicester, United Kingdom), shown in Figure

4.3. This device is equipped with a transducer that uses a standard stylus, mounted on the measurement stand column, to evaluate flat surfaces. The stylus has a diamond tip with a radius of 2 μm and an angle of 60°, and the applied force is less than 1 mN. The software used for data analysis is Metrology 4.0, and the measurement stand column moves along the Z-axis.

Figure 4.3 The device used for roughness determination

The Ra parameter represents the arithmetic mean of the absolute deviations of the roughness profile from the median line.

$$R_a = \frac{1}{l}\int_0^l |z(x)|\, dx$$

- Where l is the base length of the roughness profile.

The Rq parameter, known as the root mean square (RMS) of deviations from the median line, is more sensitive to the peaks and valleys of the profile, making it widely used in the optical industry. It generally provides a higher value than Ra.

$$R_q = \sqrt{\frac{1}{l}\int_0^l z^2(x)\, dx}$$

The Rt parameter refers to the maximum height difference between the highest and lowest points of the profile over the entire evaluation length.

Rz represents the maximum profile height and is calculated as the arithmetic mean of the five highest peaks and the five lowest valleys along the reference length, relative to a median line parallel to the profile.

$$Rz = \frac{(R_1 + R_2 + R_3 + R_4 + R_5) - (R_6 - R_7 - R_8 - R_9 - R_{10})}{5}$$

Rsk indicates the asymmetry of the distribution of deviations from the mean. A perfectly symmetrical distribution has an Rsk of 0, while a higher value indicates significant skewness in the positive or negative direction. A high positive Rsk signals the presence of sharp, thin peaks, whereas a high negative Rsk indicates narrow surface grooves. In such cases, other measurements like Ra may become less relevant.

Rku measures the kurtosis of the distribution. A high kurtosis distribution has a sharper peak and flatter edges, while a low kurtosis distribution has a rounded peak and wider edges. By definition, a normal distribution has a kurtosis of 0.

All the presented roughness parameters were determined for each anodized screw.

4.2.3. DETERMINATION OF WETTABILITY

Wettability analyzes how a liquid applied to a solid (or liquid) substrate spread or the ability of liquids to form boundary surfaces with solid states. The contact angle provides information about the interaction energy between a solid and a liquid. The smaller the contact angle or surface tension, the greater the tendency for wetting.

In this doctoral thesis, contact angle measurements were performed using the KRUSS DSA 30 system (Hamburg, Germany), utilizing three different liquids: water, diiodomethane, and ethylene glycol (Figure 4.4). Due to the complex geometry of the samples, droplets were manually applied using micrometric syringes for each liquid.

Figure 4.4. KRÜSS DSA30 Drop Shape Analysis system used for the determination of contact angle

4.3. EVALUATION OF SURFACE PROPERTIES OF ANODIZED OSTEOSYNTHESIS SCREWS

4.3.1. MICROSTRUCTURAL CHARACTERIZATION THROUGH SCANNING ELECTRON MICROSCOPY (SEM) AND ELEMENTAL COMPOSITION (EDS)

The results of the scanning electron microscopy (SEM) analysis of the anodized samples are illustrated in Figure 4.5. SEM studies were conducted on the surface to observe the topography of the analyzed samples. At first glance, significant differences in topography can be observed, which may be associated with the thickness of the anodized layer.

For the gray screw (with a layer thickness of up to 25 μm), shown in Fig. n.a, deep and shallow grooves oriented in the same direction can be observed, likely resulting from a surface preparation step before anodization.

As the layer thickness increases, fewer surface defects are visible (Fig. n.b for the blue screw, with a layer thickness between 25-50 μm), and at greater thicknesses (violet, 75-100 μm, Fig. n.c, and green, 100-125 μm, Fig. n.d), the surface topography is dominated by the specific structure of the anodized layer, formed by groups of nanotubes.

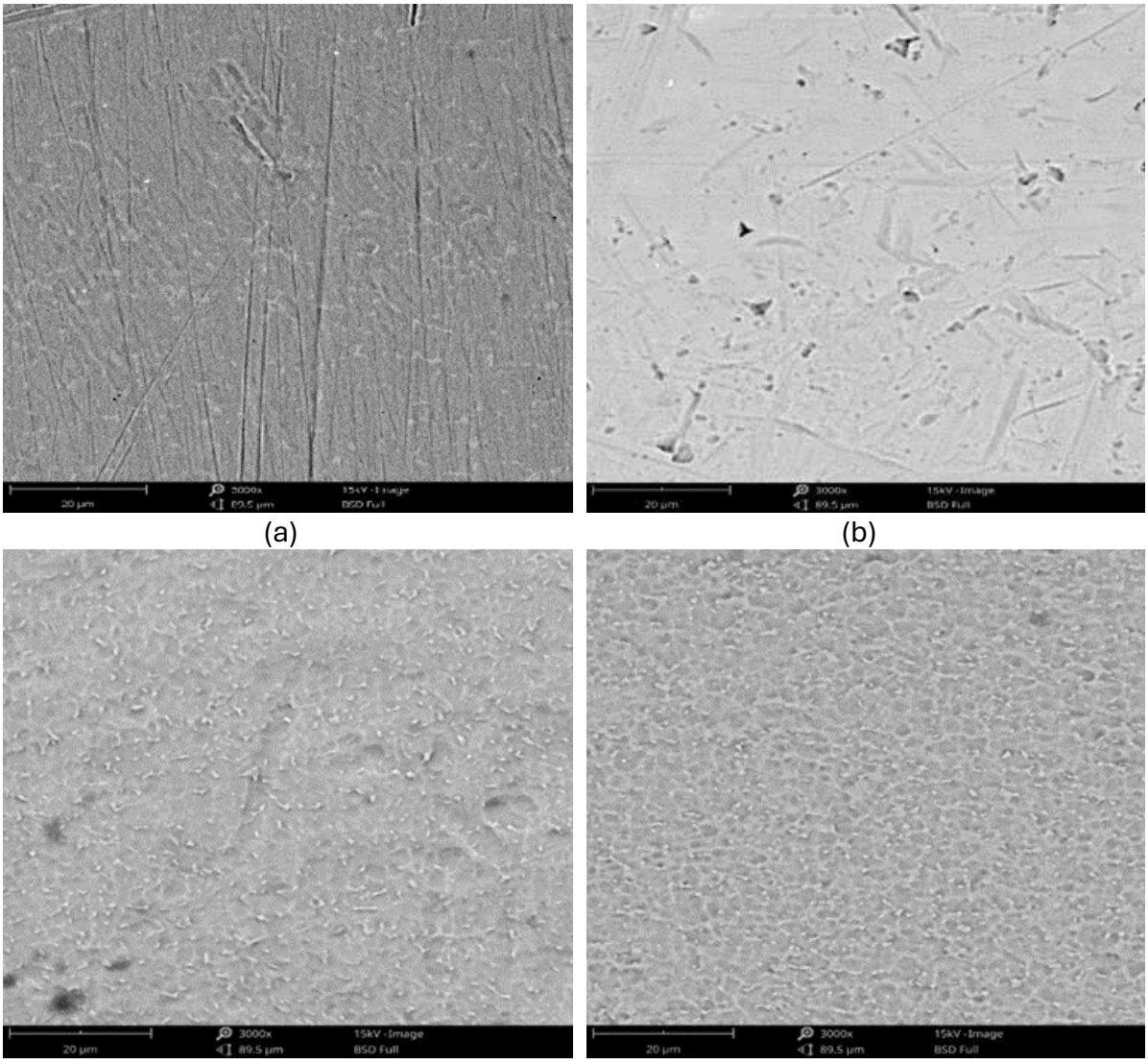

Figure 4.5. The microstructure of the analyzed titanium alloy samples observed through scanning electron microscopy: a - gray anodized screw, b – blue anodized screw, c – violet anodized screw, d – green anodized screw

Based on the analyses performed using scanning electron microscopy (SEM), it is concluded that the anodizing duration is one of the most determining factors influencing both the surface morphology and the thickness of the formed layer [93,94,95].

The surface's chemical composition was determined through energy-dispersive spectroscopy (EDS), quantifying the presence of titanium, aluminum, and vanadium—essential elements of the alloy. Additionally, the presence of oxygen was considered, given that the formed layer is titanium dioxide.

A decrease in the concentration of titanium, aluminum, and vanadium is observed as the layer thickness increases. This seems to be influenced by the changing relative position of

the electron beam's interaction volume with respect to the substrate. The interaction volume, which is teardrop-shaped, varies between 100 nm and approximately 5 µm within the surface, and as the layer becomes thicker, the information obtained from the substrate becomes more limited.

Regarding the estimated oxygen concentration, an increasing trend was observed with the layer's thickness, although no direct correlation could be established.

4.3.2. RESULTS OF ROUGHNESS INVESTIGATIONS

Surface roughness was analyzed as it is considered a crucial factor in the osseointegration process and can be regarded as an influencing factor for wetting behavior. Figure 4.7 presents selected profiles for the analyzed samples, based on the roughness parameters: arithmetic mean roughness (Ra), maximum profile height (Rz), maximum height difference between the highest and lowest points of the profile (Rt), kurtosis (Rku), skewness parameter (Rsk), and root mean square roughness (Rq).

Probe 1 - gray anodized screw

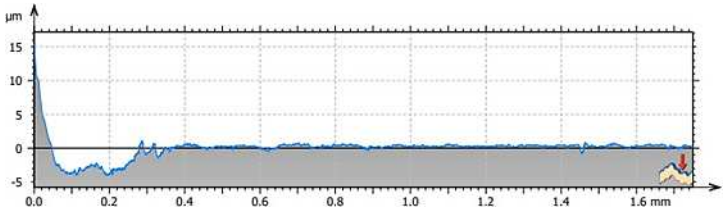

Rq	0.9846 µm
Rsk	-2.6010
Rku	8.7095
Rt	5.0385 µm
Rz	1.5591 µm
Ra	0.6044 µm

Probe 2 - blue anodized screw

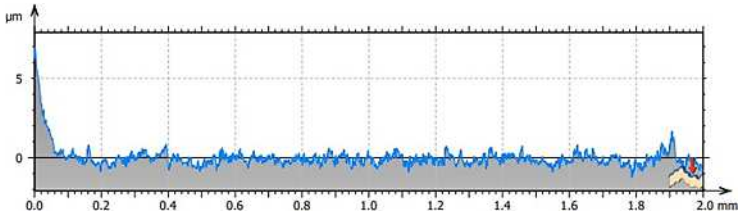

Rq	0.6937 µm
Rsk	5.3437
Rku	42.3125
Rt	8.2519 µm
Rz	2.4954 µm
Ra	0.3532 µm

Probe 3 - violet anodized screw

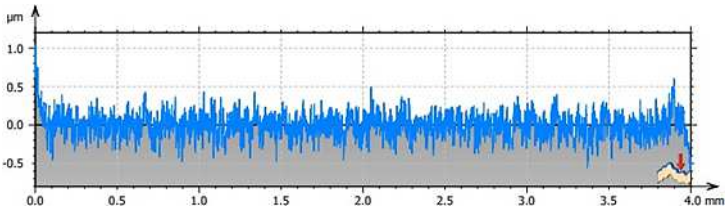

Rq	0.1569 µm
Rsk	0.3313
Rku	4.9449
Rt	1.6736 µm
Rz	0.8508 µm
Ra	0.1206 µm

Probe 4 - green anodized screw

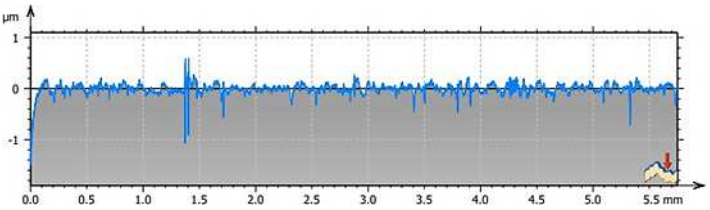

Rq	0.1134 µm
Rsk	-3.8592
Rku	39.0299
Rt	2.0897 µm
Rz	0.5533 µm
Ra	0.07 µm

Figure 4.7. Roughness analysis results of the samples

The symmetry parameter (Rsk) provides information about the height distribution of surface peaks. A negative value (below 0) indicates the presence of deep valleys on the surface, while a positive value suggests a predominance of higher peaks. The anodized screws in blue and violet showed a positive Rsk value, indicating that the peaks exceed the median line. In contrast, the gray and green anodized screws displayed Rsk values suggesting the presence of deep valleys on the surface. Furthermore, a higher Ra value associated with an Rsk close to zero suggests a balanced distribution between peaks and valleys, which is favorable for optimal osseointegration.

The Ra and Rq values show a decreasing trend as the coating thickness increases, indicating a smoother surface. Similarly, Rt decreases with increasing coating thickness, suggesting a reduction in the differences between the highest peak and the deepest valley, confirming a smoothing of the surface. This aspect is also reflected in the decrease of Rz values. According to Rsk, the height distribution is most symmetrical for a layer with a thickness of 75–100 µm (violet anodized screw), supported by the minimal Rku value, indicating the presence of less pronounced peaks and valleys. Based on the Rsk and Rku values, a layer thickness of 75–100 µm, as seen in the violet anodized screw, would generate a surface with fewer undulations, observations corroborated by SEM analyses.

4.3.3. RESULTS OF WETTABILITY THROUGH CONTACT ANGLE METHOD

The contact angle is important because it influences cell adhesion, integration with bone tissue, and the healing process of fractures. It is well known that cell proliferation and adhesion are enhanced on a hydrophilic surface with a low contact angle value ($\theta < 90°$).

The angle formed at the intersection of the liquid-solid and liquid-vapor interfaces is known as the contact angle. To determine this angle, sessile drops were applied to each sample in various regions, and 14 measurements were conducted for each sample and liquid. Similar to the surface roughness results, the contact angle decreased as the layer thickness increased when water was used as the liquid. A comparison of the contact angle with water was conducted using the ANOVA method with $\alpha=0.05$, and the results showed that the differences between the contact angles are statistically significant, suggesting that layer thickness plays an important role in wettability. A pronounced hydrophilic character can be observed.

For diiodomethane and ethylene glycol, it was observed that contact angles are higher for samples 1 (gray anodized screw), 3 (violet anodized screw), and 4 (green anodized screw), while for sample 2 (blue anodized screw), lower values were recorded. This suggests a possible modification in the chemical composition of the contact surface, possibly caused by the electrolyte used in the anodization process.

The surface free energy does not vary significantly, except for sample 2, which shows lower energy, likely due to anomalies in the contact angles for diiodomethane and ethylene glycol caused by a change in the surface chemical composition. Statistical analysis using the ANOVA, Tukey, and Fisher methods with $\alpha = 0.05$ indicates that the values are statistically significantly different, with the Tukey and Fisher tests showing that variations in surface free energy are not statistically significant for samples 1, 3, and 4, except for sample 2.

Chapter 5: DEVELOPMENT OF AN EXPERIMENTAL ANALYSIS PROTOCOL FOR METALLIC IMPLANTS USED IN TRAUMATOLOGY AFTER THEIR FAILURE

Objective of the Study, Experimental Materials, and Work Plan

This subchapter of the doctoral thesis investigates the factors that contributed to the failure of a Gamma nail used for the fixation of proximal fractures. The titanium alloy Ti6Al4V is preferred in the manufacturing of Gamma nails due to its ideal properties for orthopedic use, including excellent biocompatibility, superior corrosion resistance, and remarkable mechanical characteristics. It is important to note that the Gamma nail was explanted after a period of six months from the body of a female patient to identify the factors that contributed to its failure.

The work plan was organized into stages based on the knowledge acquired and information obtained from the specialized literature, schematically presented as follows:

- **Macroscopic characterization** through macrography and stereomicroscopy;
- **Microstructural characterization** of the implant using optical microscopy (OM) and scanning electron microscopy with energy dispersive spectroscopy (SEM-EDS) to identify the mechanisms that led to the failure of the intramedullary nail.

Table 8. Characterisation methods and utilised equipment

Objective	Method	Equipment
Macroscopic characterisation	Macrofotography	Canon DSLR camera equipped with a 90 mm F 2.8 macro lens (Canon Inc., Tokyo, Japan)
	Stereomicroscopy	Compact stereomicroscope Olympus SZX7 (Olympus Corporation, Tokyo, Japan)
Microsctructural characterisation	Optical microscopy (OM)	For this purpose, an Olympus BX51 optical microscope was used (Olympus Corporation, Tokyo, Japan)
	Scanning electron microscopy(SEM)	Philips scanning electron microscope, model ESEM XL 30 TMP

Elemental composition	Energy-dispersive X-ray spectroscopy (EDS)	Energy spectrometer EDAX (Koninklijke Philips N.V., Amsterdam, Netherlands)

5.1. METHODS OF ANALYSIS AND EQUIPMENT USED

To analyze orthopedic explants of the centromedullary rod type, stereomicroscopy, optical microscopy, and scanning electron microscopy were employed to investigate the causes and mechanisms of fracture. Following experimental determinations, the anticipated results are outlined in Table 9.

Table 9. The anticipated results to be obtained following experimental determinations, based on the research method used.

Method	Estimated results
Patient medical data	Patient clinical examination, history and bone structure information
Radiological images study	Bone and implant view
EDS Microscopy	Elemental composition determination
Macroscopical analysis through macrophotography and stereomicroscopy	Failure mechanism identification. Implant surface defect observation
Optical microscopy	Alloys and potential structural defects microstructural characteristics identification
Scanning electron microscopy (SEM)	Implant failure mechanism identification. Surface defects observation, considerations about the failure type. Identification of potential structural defects in the failure area

In the following section, the principles of the methods and equipment used in the experiments will be briefly presented.

Macrophotography

For the macroscopic evaluation of the explant, macrophotography techniques were initially employed. The images were captured using a Canon DSLR camera equipped with a 90 mm F/2.8 macro lens (Canon Inc., Tokyo, Japan), to obtain high-resolution details of the studied surfaces (Figure 5.1).

Figure 5.1. The DSLR camera used to obtain the macroscopical images

Stereomicroscopy

The stereomicroscope is a device used to observe opaque, translucent, and transparent objects under transmitted light, providing a three-dimensional view. It is ideal for various fields, such as biological, biochemical, medical, metallographic research, and electronics, making it essential for observing relief details. Unlike an optical microscope, the stereomicroscope is designed for different purposes and features two optical paths with two objectives and two eyepieces, offering slightly different perspectives for the left and right eyes, thereby creating a three-dimensional image of the examined object.

This type of stereomicroscope stands out for its performance due to its combination of modularity and optical quality. Equipped with infinity-corrected optics and a 7:1 zoom ratio, the Olympus SZX7 model provides detailed images with a resolution of up to 600 lines/mm. The ComfortView eyepieces ensure fast and comfortable use, while the QuickPHOTO software facilitates the acquisition, storage, and processing of captured images. Stereomicroscopes use reflected light (episcopic illumination), enabling the examination of thick or opaque object surfaces that cannot be analyzed with transmitted-light (diascopic)

microscopes. Additionally, they can use transmitted light, integrating a light source or a mirror under a transparent stage where the sample is placed.

Stereomicroscopy was performed using a compact Olympus SZX7 stereomicroscope (Olympus Corporation, Tokyo, Japan), shown in Figure 5.2.

Figure 5.2. Olympus SZX7 Stereomicroscope

Optical Microscopy (OM)

In this analysis, the microstructural characterization of the titanium alloy implant (Ti6Al4V) was carried out using optical microscopy.

Optical microscopy is the most used method for analyzing the microstructure of materials, allowing the observation of morphological details at magnifications between 10× and 2500×, corresponding to sizes of 0.1–1000 μm. By examining a properly prepared material, at magnifications from approximately 100× to several thousand times, the component phases, grain structure, phase and grain distribution, as well as grain size, can be identified. Considering the opacity of metallic implants, the ideal optical microscopes for analyzing orthopedic implants are metallographic ones, which use reflected light for specimen examination.

To perform optical microscopy analyses, experimental samples must be prepared through a series of rigorous steps. The first step involves cutting samples from specific areas of interest for investigation. This is followed by the embedding process, which protects the samples and facilitates their handling.

After embedding, the surface of the samples is subjected to grinding with metallographic papers, aiming to achieve a perfectly flat surface, essential for precise analysis. Subsequently, the samples are polished to attain a “mirror” finish, enhancing the clarity of the image.

Finally, a metallographic etching is applied using chemical reagents, a process intended to highlight the structural constituents of the material, allowing a detailed evaluation under the microscope. Optical microscopy analysis was performed using an Olympus BX51 microscope (Figure 5.3).

Figure 5.3. Olympus BX51 Optical Microscope

Scanning Electron Microscopy (SEM) and Energy Dispersive X-ray Spectroscopy(EDS)

Scanning electron microscopy is particularly effective for analyzing the fractured surfaces of implants. This type of microscope enables the acquisition of magnified images of samples using an electron beam, thereby facilitating the detailed examination of very small objects. An additional advantage of this technique is its ability to focus on different levels of the sample's surface at various heights, as well as its capability to determine the chemical composition of surfaces.

For these analyses, a Philips scanning electron microscope, model ESEM XL 30 TMP, equipped with an EDAX energy spectrometer (Koninklijke Philips N.V, Amsterdam, Netherlands), was used, as shown in Figure 5.4.

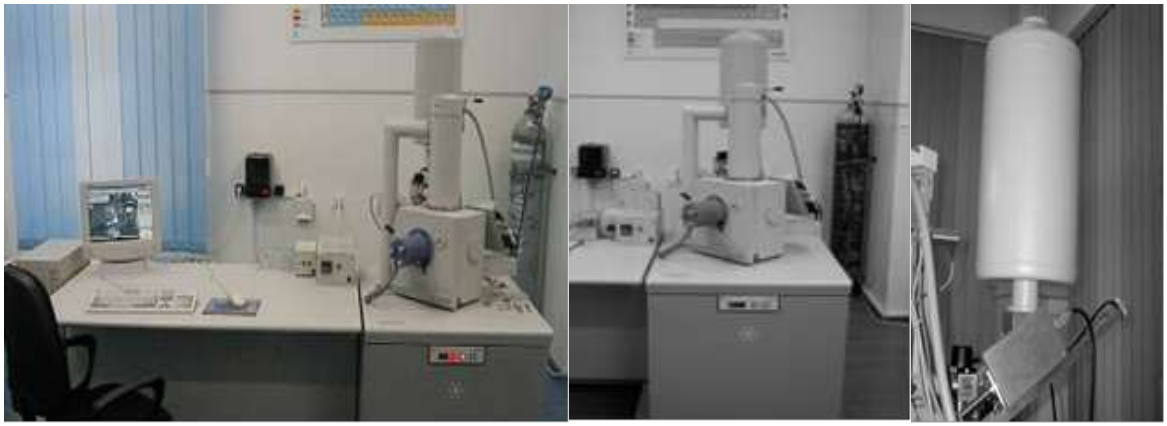

Figure 5.4 Philips scanning electron microscope model ESEM XL 30 TMP, equipped with an EDAX energy spectrometer

5.2. CASE STUDY ON THE CLINICAL HISTORY OF GAMMA NAIL FAILURE

A 69-year-old female patient, who suffered multiple injuries in a road accident, was treated with a Gamma nail for stabilizing a trochanteric fracture of the right femur. The surgical intervention involved the use of a Gamma 3 locking nail with dimensions of 11 × 180/125°, combined with a lag screw, a distal locking screw with a diameter of 3.5 mm, and an anti-rotation cap.

Six months after the intervention, the patient experienced pain and reduced mobility in the right hip. These symptoms are attributed to the lack of fracture consolidation, which may compromise the implant's integrity. These issues are illustrated in the presented X-ray (Figure 5.6).

Figure 5.6 Radiographic images showing the implant deterioration (blue arrow) and the absence of bone healing (yellow arrow)

Following the radiographic evaluation, it was decided to remove the implant and replace it with a dynamic condylar screw (DCS) system. After the Gamma nail was removed, it underwent experimental analyses to determine the causes of its functional failure.

5.3 Experimental analysis of a failed Gamma nail

Macrophotography results

Figure 5.7 illustrates, at a macroscopic level, the implant after extraction, providing an overall view of its condition. The failure point is highlighted by the blue arrow. The causes of the failure may be attributed to the presence of cracks, structural deformations, or corrosion.

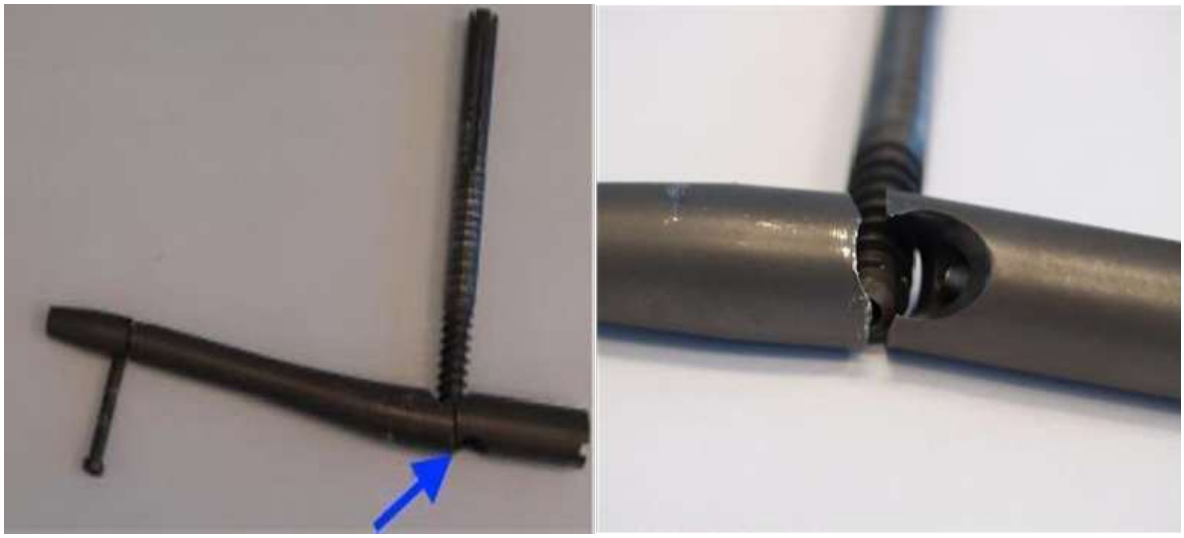

(a) (b)

Figure 5.7 The removed implant. The blue arrow indicates the point of failure. (a) Macroscopical examination after implant removal. (b) Highlighting of the failure point

Stereomicroscopic Analysis

Following the stereomicroscopic analysis of the implant's failure surface, the characteristics of the fracture zones can be observed, as illustrated in Figure 5.8. The component exhibits a low and constant energy fracture, highlighted by the presence of propagation lines, followed by a sudden final rupture. The intergranular fracture has a matte appearance and tends to form three distinct zones: the initial zone, the propagation zone, and the sudden, final rupture zone, which occurred over a short period of time (Figure 5.8-a).

In Figure 5.8-b, the fatigue fracture is emphasized, which also occurred over a short period. The failure shows a combination of fracture types, both ductile (1) and brittle (2). In Figure 5.8-c, an intergranular fracture covered by a thin layer of oxides can be observed. The details of the area reveal a cup-and-cone fracture type (Figure 5.8-d).

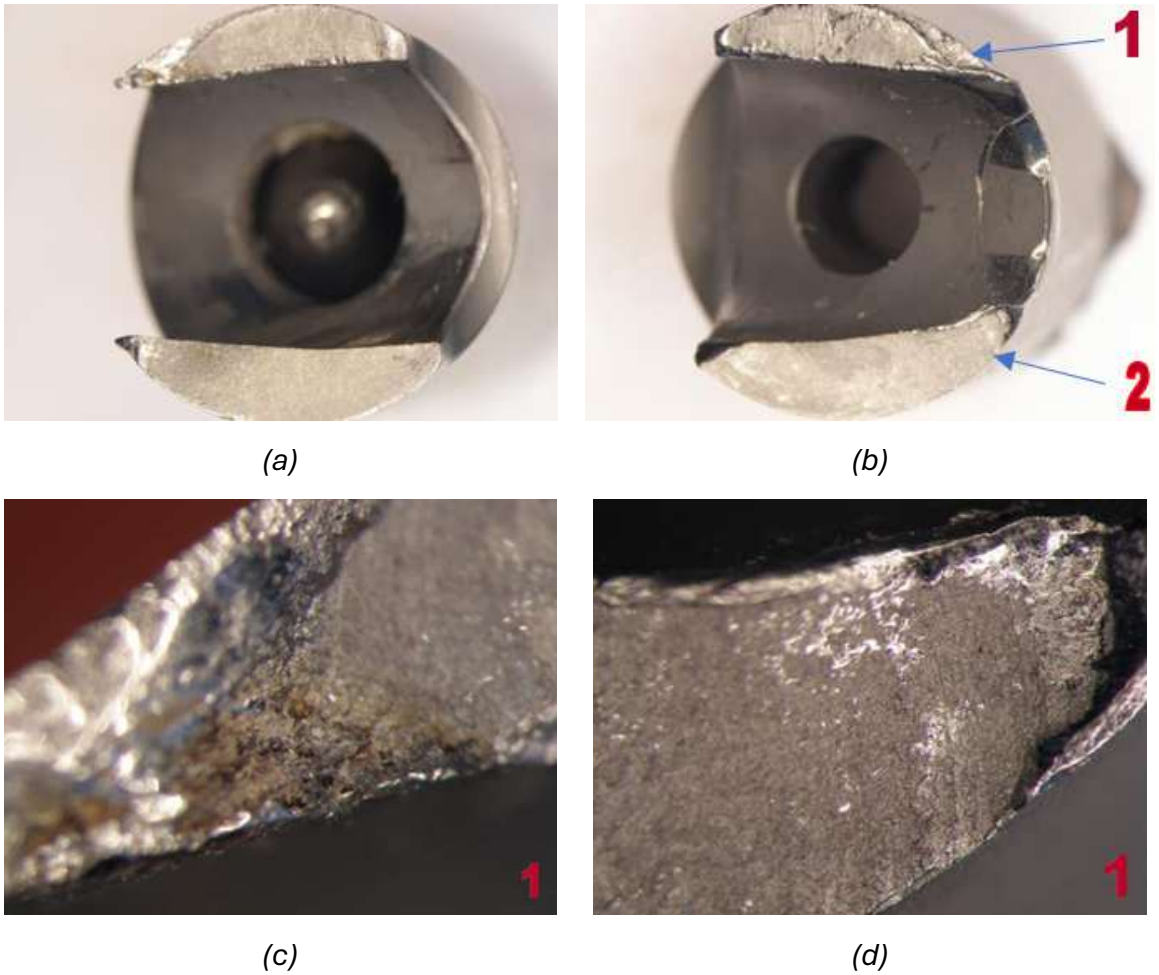

(a) *(b)*

(c) *(d)*

Figure 5.8. Stereomicroscopic images of the failure area

Preparation of Experimental Ti6Al4V Alloy Samples for Metallographic Examination

During the sampling for metallographic analysis, both the optimal sampling location and the cutting method were considered. To best highlight the structure of the implant and any structural variations, the samples were collected from areas immediately adjacent to the fracture. For optical microscopy, sampling was performed from areas unaffected by failure.

The cutting was performed using a Buehler IsoMet4000 device (Buehler, IL, USA) equipped with a special abrasive disc designed for titanium alloys and then the samples were embedded using the Remet Evolution IPA40 device which can be used for mounting samples with a wide variety of phenolic resins suitable for hot embedding.

Embedding parameters are presented in Table 10. At the end of the process, the samples were rinsed with water to remove any traces of abrasive or metallic dust, then dried by wiping.

Table 10. Embedding parameters of the experimental probes

Embedding parameters	
Heating time = 8 min	Temperature = 180 °C (350 °F)
Cooling time = 13 min	Phenolic resin
Pressure = 4 atm	Case size = 40 mm

The grinding process aimed to achieve a perfectly flat surface, free of scratches. Grinding and polishing of the samples were performed using a Buehler Beta & Vector Grinder-Polisher device (Buehler, IL, USA), shown in Figure 5.11. The grinding process was carried out according to the parameters specified in Table 11, using CarbiMet2 hydrophilic metallographic paper under a continuous flow of water. At the end of the procedure, the sample was rinsed with clean water to remove any residual abrasive metallic dust and subsequently dried by wiping.

Figure 5.11 Buehler Beta & Vector Grinder – Polisher

Table 11. Grinding parameters for the experimental Ti6Al4V samples.

Polishing Parameters						
	Polish 1	Polish 2	Polish 3	Polish 4	Polish 5	Polish 6
Time [min]	3	3	3	3	3	3
Force of application [Lb/N]	6	6	6	6	6	6
Carbi-Met particle [particles/inch]	400	600	800	1000	1200	2500

Polishing aimed to achieve a perfectly flat surface with a reflective finish. The quality of smoothing was verified under a microscope at 100× magnification, where possible non-metallic inclusions, cracks, or preparation defects were identified. To ensure surface uniformity, the sample was constantly rotated in the direction opposite to the disc's rotation, thus preventing the appearance of unpolished areas that may appear as shadows due to the presence of hard constituents. After achieving the desired shine, the sample was rinsed with water, degreased with alcohol, and dried with warm air.Unlike grinding, which involves surface abrasion, mechanical polishing reduces roughness through plastic deformation of the material, leading to the formation of a thin amorphous layer known as the Beilby layer, which can distort or obscure the sample's true structure. This layer is largely removed through chemical etching, which highlights the material's structural constituents. The parameters used for polishing the experimental samples are detailed in Table 12.

Table 12. Polishing parameters of the experimental probes

	Polish 1	**Polish 2**	**Polish 3**
Time [min]	10	10	**10**
Force of application [LB/N]	6	6	**6**
Material	Tex Met Felt	Tex Met Felt	**Tex Met Felt**

Polishing agent	Topol 1*	Topol 2**	Topol 3***

The metallographic etching aims to highlight the structural constituents. Its structure becomes visible by exposing the surface to chemical reagents, mainly acidic solutions. In the case of experimental samples made from the Ti6Al4V alloy, they were chemically etched with a solution composed of 100 ml of HF and 90 ml of distilled water. The sample was immersed in the solution for 40 seconds, then washed with water and dried with warm air. The images of the experimental samples before and after preparation are shown in Figure 5.12.

(a) (b)

Figure 5.12. Samples before processing (a). Samples after cutting, embedding, grinding, polishing, and chemical etching (b).

The images obtained using the optical microscope, shown in Figure 5.13, reveal a classic biphasic α+β structure, most likely resulting from a quenching heat treatment. The elongated shape of the grains is attributable to the plastic deformation processes that the material underwent (Figure 5.13.a-d).

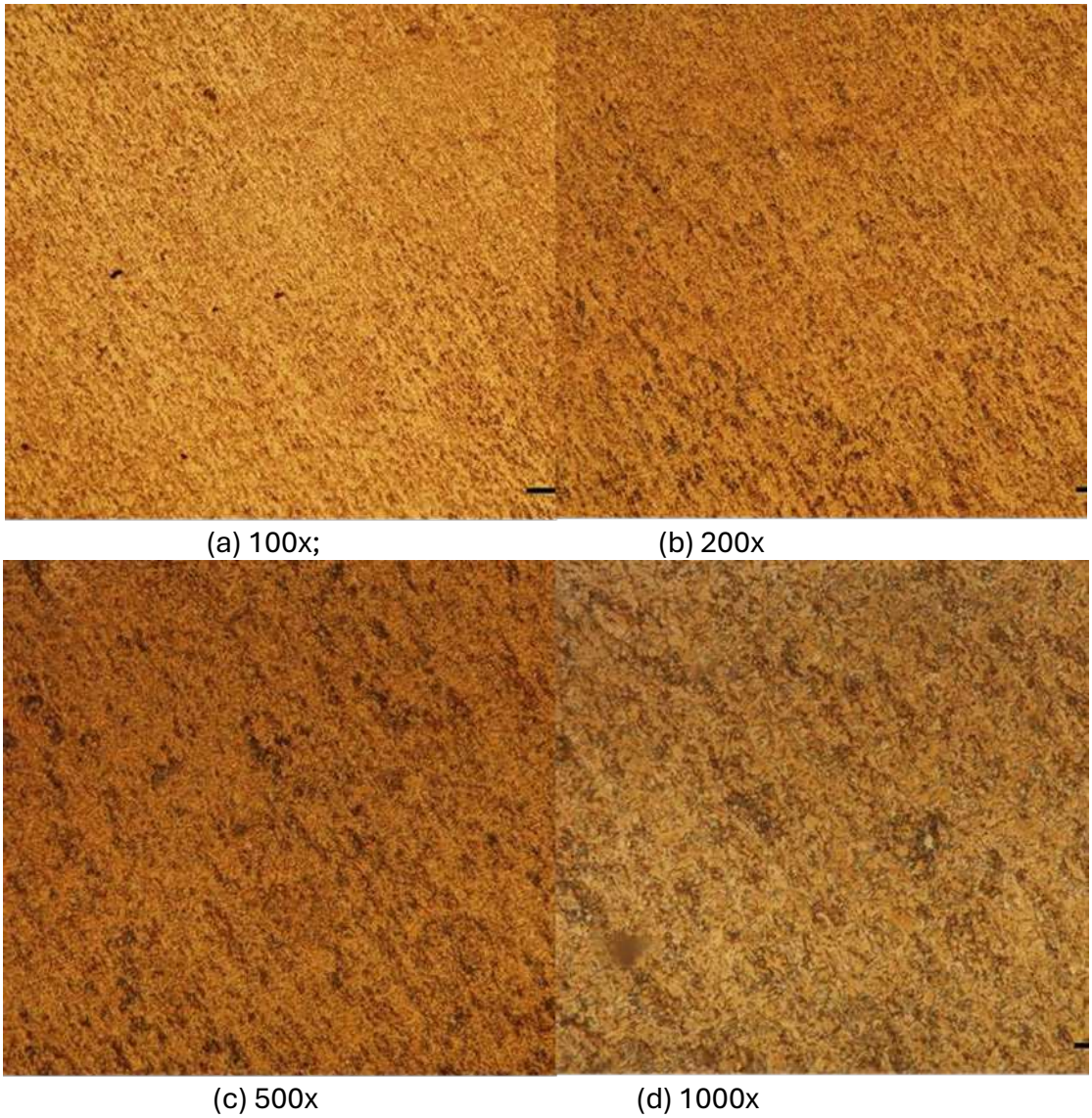

(a) 100x; (b) 200x

(c) 500x (d) 1000x

Figure 5.13. Optical microscopy images at different magnifications related to the microstructural characteristics of the implant, specifically the Ti6Al4V alloy.

Microstructural and compositional characterization by scanning electron microscopy (SEM) coupled with EDS spectrometry

In Figure 5.14-a, the intergranular fracture zone with a matte appearance, covered by a thin oxide layer (1), can be observed, highlighting the cup-and-cone characteristics of the fracture (2), as well as its propagation lines (3). In image b, intergranular fracture zones with small voids and oxides are visible on the coated sample's surface. The mixed fracture nature, at a magnification of 100x, is noticeable through the presence of brittle (1) and ductile (2) fracture zones in image c. Image 5.15-d shows a fracture magnified 500x, revealing relatively uniform dimples (approximately 10 μm) of ductile fracture, as well as relatively parallel fracture zones. Image 5.15-e highlights ductile fracture characterized by the presence of cup-and-cone

features. In image 5.15-f, the fracture zone at 2000x magnification shows relatively uniform dimples (ductile fracture) and the propagation of cracks both parallel and into the depth of the sample (Figure 5.14.a-f).

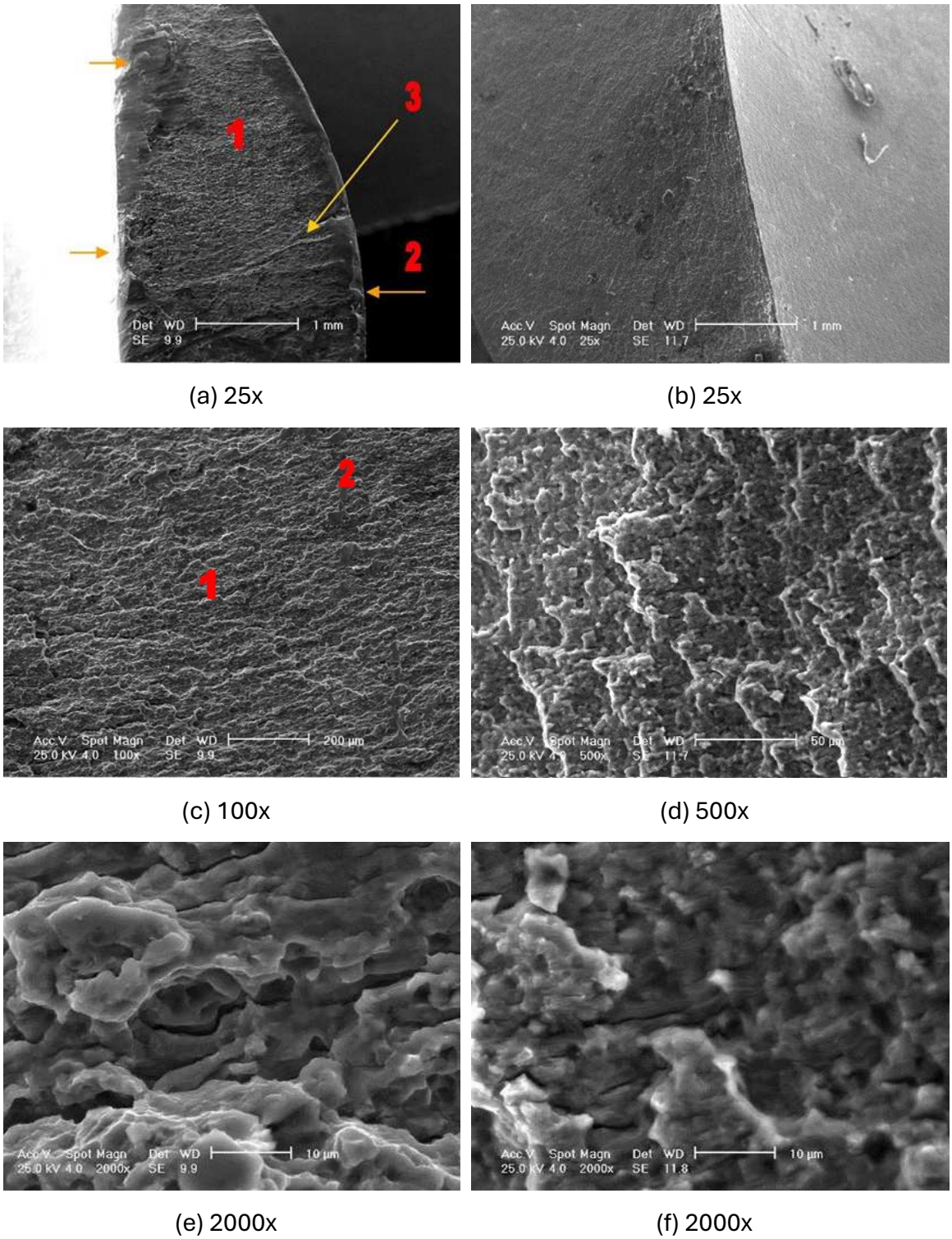

(a) 25x (b) 25x

(c) 100x (d) 500x

(e) 2000x (f) 2000x

Figure 5.14 Electronic microscope images of the failure areas

The scanning electron microscopy analyses did not reveal structural inhomogeneities in the fracture zone.

Following the quantitative and qualitative analysis performed on the failed material, along with the analysis of the X-ray emission spectrum, an evaluation of the Gamma rod's composition was conducted. It was found that the material primarily consists of titanium, aluminum, and vanadium, characteristic of Ti6Al4V titanium alloys, as shown in Figure 5.15.

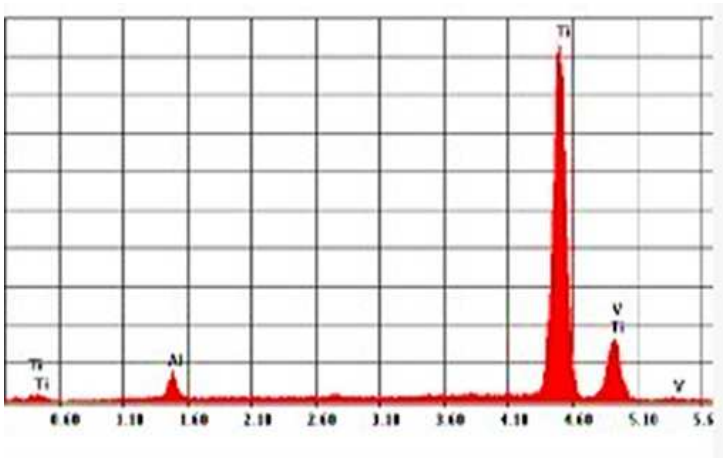

Element	wt %	at%
Ti	92,02	87,76
Al	6,38	10,80
V	1,61	1,44

Figure 5.15. EDS spectrum and compositional analysis results of the Gamma nail

The failure of Gamma nail implants can be caused by a variety of factors specific to each case. Among the most common causes is the stress concentration around the screw fixation holes, which become vulnerable points of the implant, as highlighted in the reported case. This stress concentration can initiate cracks, leading to fatigue fractures [96].

Another major cause of implant failure is the discrepancy in biomechanical criteria between the bone and the implant. Regarding manufacturing and the materials used, there are instances where implants are improperly designed or insufficiently tested prior to use. Technical errors during surgery, such as scratches and cracks occurring during placement, can also contribute to implant failure.

Proper matching of the elasticity modulus between orthopedic implants and adjacent bone, known as Young's modulus, is essential to avoid implant failure. An inadequate match, where the implant is much stiffer than the bone, can lead to bone resorption and stress shielding, increasing the risk of failure [55]. Preclinical experimental testing could allow for the

development of more compatible implants, thus offering better results in personalized treatments [97].

Regarding the discussion of implant failures, it was once believed that making implants stiffer and stronger would improve resistance to applied forces. However, it has been demonstrated that excessive implant rigidity can hinder adequate interfragmentary motion at the fracture or osteotomy site, leading to unfavorable healing and challenges in bone remodeling, as well as stress shielding. Efficient bone healing requires controlled interfragmentary motion that accounts for the characteristics of human bone [98].

Ductile and brittle failure modes represent two distinct types of structural collapse. Ductile failure involves significant deformation and energy dissipation before fracture, while brittle failure is characterized by sudden and catastrophic breakage. Ductile failure, also known as plastic deformation, occurs when the material is subjected to stresses exceeding its tensile strength limit [99]. Fracture stability influences fatigue and the stress applied to the implant, with implants tending to fail under lower loads in unstable fractures compared to stable ones, as stress on the implant increases with decreasing stability.

CHAPTER 6. CONCLUSIONS

6.1. GENERAL CONCLUSIONS

Based on the information from the specialized literature and the experimental studies conducted, the following general conclusions can be drawn:

- Magnesium alloys are potential implant materials recommended for trauma implants, as they exhibit a series of special properties far superior to conventional metallic materials, such as stainless steels and titanium alloys. These properties include an elasticity modulus close to that of human bone, better biocompatibility, and a biodegradable nature. Their biodegradability provides a major advantage in using them for temporary trauma implants, as it eliminates the need for a secondary surgery to remove them after the bone fracture heals within a few months. The only noted drawback is in clinical cases involving large fracture areas, as these materials degrade quickly, and in such cases, the fracture may not heal in accordance with the degradation rate of the implant material.
- Another highly important topic in clinical practice addressed in this doctoral thesis concerns the investigation of trauma implants following their failure in clinical practice and identifying the mechanisms and causes leading to their failure. Given the controversial situations of premature failure due to trauma implant fractures, involving orthopedic surgeons, implant manufacturing companies, and patients, establishing an investigation protocol for failed implants in correlation with clinical data and relevant medical imaging for each case is particularly important. This doctoral thesis specifically highlighted the causes of failure and the fracture mechanism of Gamma nails, as well as aspects of osteointegration in the case of Herbert screws. This thesis opens new perspectives for interdisciplinary collaboration in investigating and emphasizing the major role of implant materials in the success of surgical procedures in orthopedic surgery.

6.2. ORIGINAL CONTRIBUTIONS

Regarding the *"Evaluation of the surface properties of anodized osteosynthesis screws",* the following conclusions can be drawn:

- Anodizing titanium alloys allows osteosynthesis screws to be manufactured in various colors, thus facilitating their identification in clinical practice based on diameter and reducing the risk of selection errors during surgical procedures.
- By adjusting anodizing parameters, variations in surface properties can be achieved, directly influencing cell adhesion, integration with bone tissue, and the fracture healing process. The anodizing process can enhance the adhesion of screw-type implants to human bone by modifying the chemical and physical characteristics of their surfaces.
- The resulting color from anodizing varies depending on the applied voltage. However, it should be emphasized that this process is complex and sensitive to several factors, including electric voltage, electrolyte solution composition, anodizing duration, and the initial surface properties of the screws.
- The colors obtained are not just aesthetic or practical, as different anodizing processes induce significant variations in the surface properties of osteosynthesis screws.
- Experimental results obtained in this subsection of the doctoral thesis indicate that these properties vary considerably depending on the anodizing parameters. According to the study, an anodized layer thickness of 75-100 μm is optimal for surface roughness. Thinner layers maintain the original surface characteristics, while thicker layers generate increased roughness through a preferential growth mechanism.

Regarding the *"Surface analysis of a titanium plate implant used for humerus fracture after mechanical testing",* the following conclusions can be drawn:

- A system simulating the fixation of a fracture in a humeral defect was tested, evaluating the mechanical behavior of the system. Although the test involved a compressive load, the bone fixation plate was subjected to bending stress. Following this stress, the plate underwent plastic deformations, leading to damage to the anodized layer, and the surface characteristics in these regions were subsequently analyzed.
- Roughness parameters (Rq, Rt, Rz, and Ra) showed significant decreases in stressed regions, with Rt displaying the most considerable variation. Surface topography

changes were attributed to the flattening of peaks and valleys due to plastic deformation, confirmed by reductions in Rku and Rsk parameters, suggesting a more symmetrical distribution of peaks and valleys.

- Additionally, improved surface wettability was observed in stressed regions, correlated with an increase in surface free energy. This increase enhances surface instability, making it more prone to chemical reactions and, implicitly, more susceptible to corrosion processes.

Regarding the *"Experimental analysis of a failed Gamma nail",* the following conclusions can be drawn:

- Using microscopic equipment to determine the causes of the Gamma nail failure was essential, as it allowed the identification of the type and causes of failure. Determining the causes of failure is crucial to preventing their recurrence and identifying potential alternatives. This aspect is particularly important given the high morbidity currently associated with trochanteric fractures and the frequent need for implant replacement.
- Analyses performed using stereomicroscopy, optical microscopy, and scanning electron microscopy excluded preparation and material processing imperfections as potential causes of implant failure. The absence of inclusions and structural defects in the fracture area suggests that the implant was not the determining factor in the breakage. The fracture zone was located at the distal locking system, without signs of excessive friction or scratches on the implant surface that might have occurred during insertion.
- The analysis, combined with data from the specialized literature, showed that many cases of Gamma nail implant failures are associated with screw failures caused by mechanical stresses in a cyclic loading environment and errors in the use of guiding instruments. Moreover, proper use of surgical instruments is of critical importance. While forces exerted immediately after implantation are not critical, over time, due to repeated loading cycles, the implant's mechanical strength can diminish, leading to its failure.
- Experimental analyses using microscopic techniques validated the conformity of Gamma nails regarding their chemical composition and microstructure, highlighting that implant failure was caused by surgical technique errors. Subjected to mechanical overload, the intramedullary nail failed, displaying ductile-type fracture characteristics.

Regarding the *"Experimental analysis of a Herbert screw used for patellar fracture fixation"*, the following conclusions can be drawn:

- Titanium-based implants are a safe and effective option for treating osteochondral injuries in pediatric patients, offering clinically validated results. Considering the associated risks, it is essential to explore innovative solutions for developing bioabsorbable implants, which are better tolerated by the body and promote superior osteointegration.
- Currently, magnesium is the most widely used and discussed biodegradable material, as it does not require surgical removal, degrading gradually after being implanted in the body.
- Biodegradable implants are considered a safer option compared to conventional devices, as they are expected to enable faster patient recovery. This is particularly important for highly active categories, such as children, while avoiding risks associated with permanent implants.

6.3. FUTURE DEVELOPMENT PERSPECTIVES

This doctoral thesis suggests future directions for implant development, including design optimization, shape adjustment, and surface modifications. Furthermore, to evaluate their efficacy, the behavior of these implants can be analyzed during their integration into the human body. Comparisons with other samples will allow the benefits of design modifications and surface adaptations to be determined, including their impact on reducing healing time.

Another essential element is the proper execution of the surgical procedure, as, as mentioned earlier, this is among the main causes of implant failure. The implant can be optimized from all perspectives, but an improperly performed surgical procedure will inevitably lead to its failure over time.

SELECTIVE BIBLIOGRAPHY

55. Abd-Elaziem, W.; Darwish, M.A.; Hamada, A.; Daoush, W.M. Titanium-Based Alloys and Composites for Orthopedic Implants Applications: A Comprehensive Review. Mater Des 2024, 241, 112850, doi:10.1016/j.matdes.2024.112850.

88. Sunil Kahar, A.S.V.P.U.K. Anodizing of Ti and Ti Alloys for Different Applications: A Review. IJSRD - International Journal for Scientific Research & Development| 2020, 8, 2321–0613.

93. Velten, D.; Biehl, V.; Aubertin, F.; Valeske, B.; Possart, W.; Breme, J. Preparation of TiO 2 Layers on Cp-Ti and Ti6Al4V by Thermal and Anodic Oxidation and by Sol-gel Coating Techniques and Their Characterization. J Biomed Mater Res 2002, 59, 18–28, doi:10.1002/jbm.1212.

94. Ohtsuka, T.; Nomura, N. The Dependence of the Optical Property of Ti Anodic Oxide Film on Its Growth Rate by Ellipsometry. Corros Sci 1997, 39, 1253–1263, doi:10.1016/S0010-938X(97)00025-5.

95. Yilmaz, O.; Ebeoglugil, M.F.; Dalmis, R.; Dikici, T. Effect of Anodizing Time on the Structural Color and Photocatalytic Properties of the TiO2 Films Formed by Electrochemical Method. Mater Sci Semicond Process 2023, 167, 107768, doi:10.1016/j.mssp.2023.107768.

96. Okazaki, Y.; Gotoh, E.; Mori, J. Strength–Durability Correlation of Osteosynthesis Devices Made by 3D Layer Manufacturing. Materials 2019, 12, 436, doi:10.3390/ma12030436.

97. Dichio, G.; Calì, M.; Terzini, M.; Putame, G.; Zanetti, E.M.; Costa, P.; Audenino, A.L. Engineering and Manufacturing of a Dynamizable Fracture Fixation Device System. Applied Sciences 2020, 10, 6844, doi:10.3390/app10196844.

98. Mori, Y.; Kamimura, M.; Ito, K.; Koguchi, M.; Tanaka, H.; Kurishima, H.; Koyama, T.; Mori, N.; Masahashi, N.; Aizawa, T. A Review of the Impacts of Implant Stiffness on Fracture Healing. Applied Sciences 2024, 14, 2259, doi:10.3390/app14062259.

99. Moore, P.; Booth, G. Failure Modes and Analysis in Metals. In The Welding Engineer s Guide to Fracture and Fatigue; Elsevier, 2015; pp. 95–110.